# Concrete filled rectangular steel hollow section columns subjected to major axis bending - experimental and numerical study

Abdel-Kareem Al-Rawdan
*Civil Engineering Department, Faculty of Engineering, Mutah University, Jordan*
*akrodan@mutah.edu.jo*

Tests were carried out on nine composite columns of 3m approximate length. The columns were made of concrete-filled 150x100x5mm and 120x80x5mm rectangular steel hollow sections and subjected to uniaxial bending about the major axis. This paper also describes the application of the commercially available non-linear general-purpose finite element package ABAQUS to study the behaviour of concrete-filled rectangular hollow sections. The results of these tests are reported and are compared with the predictions of the British Standard BS5400 and the finite element results. These studies provide particular insights into key aspects of the behaviour of concrete-filled rectangular hollow sections that would not have been possible using the experimental approach alone.

يعرض هذا البحث النتائج التي تم الحصول عليها من جراء اختبار تسعة أعمدة مركبة بطول ٣ أمتار. والأعمدة مصنوعة من قطاعات مستطيلة من حديد مفرغ معبأ بخرسانة بمقاسات مختلفة ١٢٠x٨٠x٥٠ و ١٥٠x١٠٠x٥ و معرضة لعزم انحناء أحادى حول المحور القوي. كما يعرض البحث أيضا لاستخدام طريقة العناصر المحددة اللاخطية لدراسة هذا النوع من الأعمدة باستخدام برنامج تحليل إنشائي تجاري متوفر. و تم مقارنة النتائج المعملية مع نتائج معادلات الكود البريطاني(BS٥٤٠٠) و أيضا مع النتائج العددية و توفر الطرق العددية إيضاحات و معلومات كثيرة لسوك هذه النوعية من الأعمدة المركبة قد يصعب الحصول عليها باستخدام التجارب العملية بمفردها.

**Keywords:** Concrete, Concrete-filled steel tubes, Columns, BS5400, Finite element, Uniaxial bending

## 1. Introduction

The combination of steel and concrete in the form of concrete-filled hollow section columns takes full advantage of both materials. On one hand, the steel hollow section dispenses with the need for any type of formwork for the *in situ* concrete core and also provides the tension reinforcement for the concrete core in the extreme fibers of the section, where it is most cost effective. On the other hand, the concrete core provides lateral support to the wall of the steel hollow section and thus prevents it from suffering prematurely from local instability. It also increases the load-carrying capacity of the steel hollow section at very little extra cost [1, 2]. Furthermore, under fire conditions the concrete core works as a heat sink and thus improves the fire resistance of the steel section to the extent that fire protection for the exposed steel tube might not be required [3,4].

Most of the published work available on composite columns concerns the concrete-encased type, with fewer publications on the concrete-filled type of columns [5,6]. The reason for this discrepancy is that the former type of columns was developed earlier, and the concrete encasement was originally used only as a means of protecting the structural steel section against fire. It is, therefore, believed that further tests on composite columns of concrete-filled Rectangular steel Hollow Section (RHS) are required in order to provide experimental and numerical evidence to check the validity of the existing design recommendations [7, 8].

The number of variables involved in concrete-filled composite columns is large, with the behavior of these columns being affected by the size and length of columns, eccentricity ratio $e_x/D$, the bond strength between steel and concrete and the material properties [9]. It would be expensive and time

consuming to attempt to study the problem solely on the basis of experimental testing; moreover, it is not possible to record the load-strain history and other detailed aspects of behavior for all components over their full area, specially the concrete inside the steel tube, regardless of the resources used. The non-linear finite element method may provide a better alternative to experimental testing, since it is possible to study composite column response at any required point, as well as to consider its overall features provided the model is correctly developed [10, 11].

This paper reports the finding of ongoing research on the development, validation and exploitation of FE models for the analysis of concrete filled composite columns. The work has utilized a non-linear general-purpose finite element software (ABAQUS) [12]. It has been found possible to accurately simulate the response of such columns, provided the material stress-strain curves are known e.g. for the steel tube from the relevant coupons tests. The validation has covered detailed strain histories within key areas and the load-displacements response up to and beyond failure.

Full-scale tests were carried out on nine 3m-long composite columns of concrete-filled rectangular hollow sections. Four tests were carried out on composite columns of concrete-filled 120x80x5 RHS and five tests on columns made of the larger section of 150x100x5 RHS. The columns were subjected to a uniaxial bending about the major axis with the end eccentricity ratios $e_x/D$ in the range of 0.1/0.125 to 0.5. For each of these columns, test observations included the failure loads, load-displacement response, and load-strain variation at several sections along its length. Short composite specimens were also tested in axial compression in order to establish the squash load of stub columns of this type of section. Short composite columns exhibit a failure mechanism which is characterized by yielding of steel and crushing of concrete, on the other hand for long composite columns the failure mechanism is characterized by partial yielding of steel crushing of concrete in compression and cracking of concrete in tension because the bending moment which continuously increasing as the column deforms laterally. Specimens of 450mm long were also prepared and tested to investigate the bond strength between the concrete filling and the steel section.

## 2. Material properties

Tests were carried out on tension coupons taken from the four walls of each 7.5m length of the steel RHS. Since two columns were manufactured from each 7.5m length of tubing, then each pair of columns was therefore considered to have the same properties of steel. The main results of these tests are summarized in table 1. The tabulated values are the average of the results obtained from testing the four coupons. For each column, the average values of the design strength $f_{sd}$ and elastic modulus, $E_s$, are given.

Table 1
Material properties

| Column number | $f_{sd}$ (N/mm$^2$) | $f_{cu}$ (N/mm$^2$) | $E_s$ (kN/mm$^2$) |
|---|---|---|---|
| 1xa | 334 | 47.1 | 205 |
| 2xa | 334 | 46.2 | 205 |
| 3xa | 337 | 47.3 | 206 |
| 4xa | 337 | 48.0 | 206 |
| 1xb | 348 | 46.1 | 203 |
| 2xb | 348 | 47.2 | 203 |
| 3xb | 341 | 48.0 | 204 |
| 4xb | 341 | 47.5 | 204 |
| 5xb | 352 | 48.3 | 205 |

The average design strength was found to vary from 334N/mm$^2$ to 352N/mm$^2$ and the elastic modulus $E_s$ values varied from 202kN/mm$^2$ to 206kN/mm$^2$. The obtained stress-strain relationships justified the assumption of an elastic-perfectly plastic model for the steel used. All column analysis and calculations given later are based on the $f_{sd}$ and $E_s$ values obtained from the tension coupons.

The concrete mix used throughout the tests was 1:1.9:2.4/0.55 with maximum aggregate size (river gravel) of 10mm. When each column and its associated stub columns were filled with concrete, five 100mm cubes were cast from the same concrete mix. The

cube strengths of concrete, $f_{cu}$, were taken as the average 28-day results of those tests. The test results of all cubes are given in table 1 and the $f_{cu}$ values are noted to vary from 46.1 to 48.3 N/mm².

### 3. Properties of composite section

The three main properties of a composite section are the squash load, $N_{ue}$, the ultimate moment of resistance, $M_u$, and the interaction curve of the section. The latter gives the relationships between the axial load, N, and the uniaxial moment, $M_x$ or $M_y$, which when acting simultaneously cause the section to reach full plasticity. Tests were carried out on short composite specimens to determine the squash load. For each column, one 200mm-long tube was tested in compression. These tubes 200mm-long were filled with concrete of the same mix as their respective columns, and were tested to failure with a view to evaluating the experimental squash load values, $N_{ue}$, of the composite columns. The failure mode of the specimens was a typical crushing failure mode, where at failure the steel was pushed out by the concrete core. The crushed concrete took the shape of the deformed steel section. Fig. 1 shows some of the tested squash specimens.

Table 2 gives the experimental test results of the composite stub specimens, $N_{ue}$; The table also shows the squash load values, $N_u$, predicted in accordance with equation 11.1.4, BS5400 [7]. The predicted $N_u$ values are given by the following expression in which the material partial safety factors are here taken equal to unity.

$$N_u = f_{sd} A_s + 0.67 f_{cu} A_c. \quad (1)$$

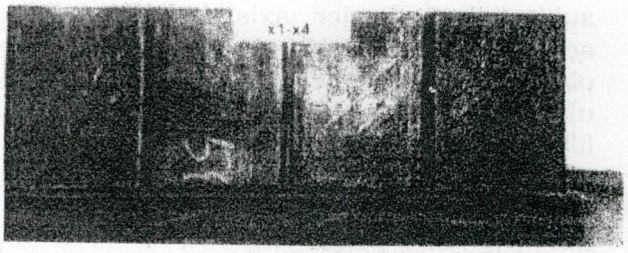

Fig. 1. Squash specimens after testing.

Table 2 shows that the experimental squash loads are generally in excess of the predicted values and that they are between 2% and 13% higher than the BS5400 predictions; equation 11.1.4 [7]. It may be concluded that the maximum compressive strength of $0.67 f_{cu}$ is a practical basis for evaluating the squash load of concrete-filled rectangular hollow sections. Nevertheless, it should be stated here that, research carried out by other researchers [1] show that the experimental failure loads are adversely affected when the height of the squash specimens is increased. However, no guidance seems to be available in the standard regarding the height of squash specimens relative to the lateral dimensions of the composite section.

Table 2
Carrying capacities of short column sections

| Specimen for column | $e_x$ (mm) | Squash load (kN) | | $N_{ue}/N_u$ | Ult. moment of res. (kNm) | |
|---|---|---|---|---|---|---|
| | | $N_{ue}$ | $N_u$ | | $M_{ux}$ | $M_{uy}$ |
| 1xa | 15 | 901 | 877 | 1.03 | 27.7 | 20.4 |
| 2xa | 30 | 893 | 872 | 1.02 | 27.7 | 20.4 |
| 3xa | 45 | 998 | 884 | 1.13 | 28.0 | 20.0 |
| 4xa | 60 | 930 | 887 | 1.05 | 28.0 | 20.6 |
| 1xb | 15 | 1311 | 1224 | 1.07 | 46.7 | 34.3 |
| 2xb | 30 | 1326 | 1233 | 1.08 | 46.8 | 34.3 |
| 3xb | 45 | 1292 | 1223 | 1.06 | 46.0 | 33.7 |
| 4xb | 60 | 1360 | 1219 | 1.12 | 45.9 | 33.7 |
| 5xb | 75 | 1332 | 1252 | 1.06 | 47.4 | 34.8 |

Series xa: 120x80x5RHS Series xb: 150x100x5RHS L = 200mm

The ultimate moment of resistance, $M_u$, of a concrete-filled section may be obtained by using the rectangular stress block for concrete and steel for the composite section shown in fig. 2. The value of $M_u$ is evaluated by first determining the position of the neutral axis of the section. This may be carried out by a trial and error procedure. When the section is subjected to major axis bending, and in accordance with BS5400, the position of the plastic neutral axis and the value of the ultimate moment of resistance of the concrete-filled rectangular hollow section my be obtained from the following expressions:

$$D_c = (A_s - 2Bt) / (b\rho + 4t), \quad (2)$$

$$M_u = f_{sd} [A_s (d - d_c)/2 + Bt (t + d_c)]. \quad (3)$$

Where $\rho$ is the ratio of the compressive strength of concrete in bending to the design strength of steel, and is given by:

$$\rho = 0.6 f_{cu} / f_{sd}, \quad (4)$$

and the rest of the symbols are as shown in fig. 1 and as given in the notation.

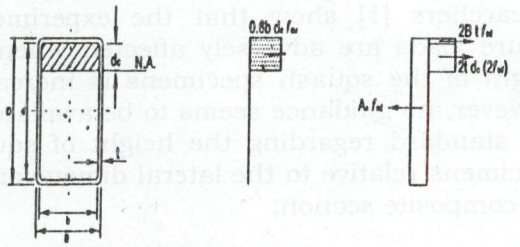


Fig. 2. Rectangular stress block.

## 4. Column specimens

As stated above two steel sections were used in these tests, i.e. 120x80x5mm RHS and 150x100x5mm RHS. The column sections and the eccentricities of the applied compressive forces are summarized in table 2. The columns were made from steel sections delivered in 7.5m lengths. Each length was cut into several pieces for the preparation of tension coupons, short composite specimens, bond specimens, and composite columns. Two 2700mm-long end pieces were tested as composite columns. Each column was provided with 15mm thick rectangular end plates which when bolted to the loading plates of the test rigs, provided the required eccentricities to the columns both ends (top and bottom-end). The end plates were welded to the column ends with 6mm-fillet weld. One of the end plates was solid, whereas the other end plate had a rectangular hole as large as the column section to enable the casting of the concrete to be carried out. When bolted to the loading plates and fitted in the test rig, each column had an effective length of 3000mm about the major axis. The initial out-of-straightness of the columns was not measured.

During the concrete casting operation, the columns were clamped to a vertical stiff column, which was secured to the strong floor of the laboratory. Vibrators were attached to the supporting column at the quarter points, and the columns were subjected to intermittent vibrations during the casting of the concrete to eliminate air pockets in the concrete and to give a homogeneous mix.

The properties of the nine columns tested are given in table 2, and include both the squash load of each column, as obtained experimentally from the squash specimens $N_{ue}$, and BS5400 predictions $N_u$. The ultimate moments of resistance about the major axis of the column section, $M_{ux}$, are also listed. It is worth mentioning here that, for the case of column subjected only to major axis bending, BS5400 requires that the column be designed for biaxial bending in which the minor axis eccentricity is taken equal to 3% of the smaller lateral dimension of the column, i.e. 3.0mm in the case of the tested columns of 150x100x5mm RHS and 2.4mm for 120x80x5mm RHS.

## 5. Bond slip specimens

For the completion of the test program nine tubes, 450mm-long cut from the RHS, and filled with concrete, were tested in order to determine the steel-concrete bond strength. These tests were carried out in association with each composite column. A gap of about 50mm high was left below the top level of the specimens when the concrete was cast to

enable the movement of the concrete core relative to the steel section during the tests. When being tested, the specimens were turned upside down, and the load was applied to the concrete core through a thick steel plate placed at the top of the specimens. Similar to the squash specimens, the steel lengths were used as received without the inside surface being treated in any way. The bond strength of the tested specimens was obtained by dividing the failure loads of the bond specimens by the area of interface of as shown in table 3. As can be seen from the table, the bond strength varied between 0.47 and 0.58N/mm²with an average value of 0.53N/mm², which is 30% greater than the value 0.4N/mm² given in BS5400. The specimens were apparently identical, and the variation in the bond strength could have been caused by different micro- and macrolocking between the concrete core and the steel surface [13]. The former depends on the surface roughness of the steel section, and the latter is related to

Table 3
Test results on bond specimens

| Specimen for column | Failure load (kN) | Length of interface (mm) | Bond strength ($N/mm^2$) |
|---|---|---|---|
| 1xa | 71 | 394 | 0.50 |
| 2xa | 82 | 397 | 0.57 |
| 3xa | 76 | 396 | 0.53 |
| 4xa | 80 | 396 | 0.56 |
| 1xb | 91 | 395 | 0.50 |
| 2xb | 86 | 396 | 0.47 |
| 3xb | 97 | 398 | 0.53 |
| 4xb | 95 | 395 | 0.52 |
| 5xb | 102 | 397 | 0.58 |

Series xa: 120x80x5RHS, Series xb: 150x100x5RHS, and L = 450mm

the frictional resistance to movement along the steel-concrete interface and is dependent on the deviations of the internal section dimensions from the true surface shape.

## 6. Test rig and instrumentation for column specimens

The tests on the column specimens were carried out on a test rig of 3000kN capacity shown schematically in fig. 3. The rig has a headroom of about 3.0m, and is securely bolted to the strong floor of the laboratory. A 3000kN capacity hydraulic jack provides the compressive force $N_e$ on the composite column. The test rig is provided with loading plate and a ball in order to allow the tested columns freedom of rotation about the required axis; fig. 4 shows detail of column end. Vertical and horizontal displacements were measured at mid-length and at the quarter points of the tested columns. This was carried out by the use of displacement transducers, which were also placed at the column ends in order to monitor any lateral displacements of the loading end plates, resulting from the flexibility of the test rig. Whitewash was applied to one half of each column specimen in order to facilitate observing the onset of yield in the steel section, and also to follow the progress of yield as the applied load was increased. Four strain gauges were fixed at the midpoints of the walls of the RHS both at mid-length and at a quarter point of each column specimen.

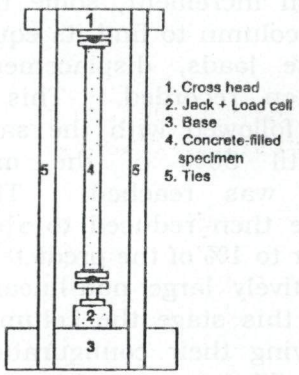


Fig. 3. Test rig and specimen.

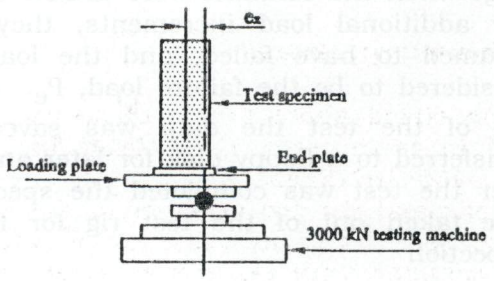


Fig. 4. Column end detail.

The load cell output, strains and displacements were all recorded using data logging equipment and all observations were

saved on disk for analysis. The mid-span strains were also plotted on a monitor during the course of the test in order to follow the load-strain relationship and also to help determine the load increment to be applied to the column specimen, especially close to failure and in the post failure stage.

## 7. Test procedure

All column specimens were vertically tested using the test rig shown in fig. 3. Each column end plate was bolted to 40mm thick loading plates that were in turn tested on rollers to allow the ends of specimens to rotate freely about both axes, and to prevent fiction at the column ends. All tests were carried out by subjecting the columns to end compressive forces applied at equal end eccentricities. The loading process started by increments of about 5% of the predicted failure load. For the first two increments, a complete check of displacements, strains and load was carried out. After each increment, some time was allowed for the column to find its equilibrium shape, and the loads, displacements and strain were then recorded. This loading procedure was followed with the same load increments until 50% of the maximum predicted load was reached. The load increments were then reduced to about 2%, and then further to 1% of the predicted failure load when relatively large non-linearity was monitored. At this stage the columns were continually varying their configuration until they were in equilibrium, therefore more time was allowed before recording any data. At the stage when the columns were unable to take any additional load increments, they were assumed to have failed, and the load was considered to be the failure load, $P_e$. At the end of the test the data was saved and transferred to a floppy disk for later analysis. After the test was completed the specimens were taken out of the test rig for further inspection

## 8. Numerical modeling of composite columns

Numerical methods, such as the Finite Element method (FE), have been found to be very convenient in the analysis of structures under static loading. The advantage of FE is that it allows the modeling of structures involving complex geometry, arbitrary loading and general material properties, and the variations of many parameters can be achieved with ease. The FE when used in conjunction with experimental methods can reduce the design cost and analysis as well as enables parameters, not easily experimentally measurable, to be monitored.

Proper modeling of a composite column requires accurate representation of all the key components, e.g. steel hollow section, concrete core, interface between steel and concrete and end plate. A realistic model should allow for slip, separation and closure at the interface of the concrete and the steel tube. The model should also allow for the buckling as well as the load-deformation response of the various components

### *8.1. Modeling of steel hollow section*

Due to the symmetry of the test specimens about column mid-height, only the upper half of the column was modeled, as shown in fig 5. Using ABAQUS library, forty shell elements with six degrees of freedom per node with eight nodes per element were used for the steel hollow section, as shown in fig. 6. The dimensions of the elements were decided after a few initial runs to test convergence, but also controlled by the degree of accuracy required and the time. The material properties were modeled by a multi-linear representation of the coupon test results.

### *8.2. Modeling of concrete and end-loading plate*

The plain concrete inside the hollow steel section was modeled by using brick elements with twenty nodes per element, as shown in fig. 7. This element was also used to model the rigid end plate through which the load on the column is applied. This element has a high calculation cost, but it gives reasonably accurate results. It has three active degrees of freedom at each node. The compressive response of concrete that was incorporated in the model is illustrated by the uniaxial response of the cube test specimens, which is

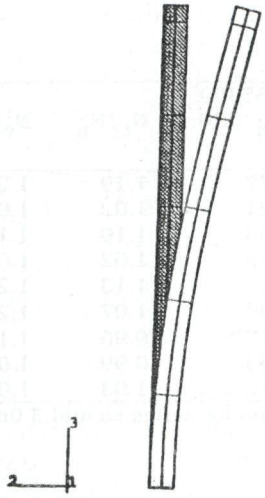


Fig. 5. Deflected shape of column.

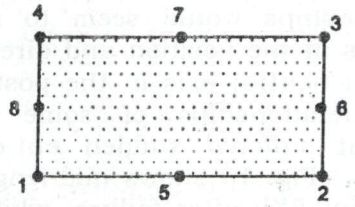


Fig. 6. Shell element (S8R).

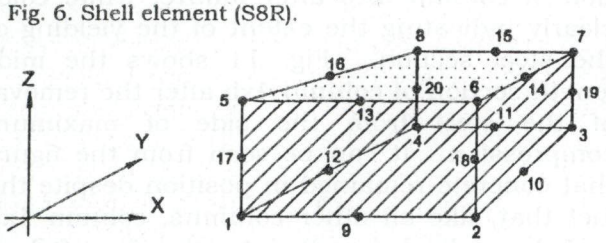


Fig. 7. Brick element (C3D20).

based on the stress-strain curve as given by BS8110. It is assumed that when uniaxial concrete specimen is loaded in tension it responds elastically until a crack forms at a stress equal to 10% of the compressive strength ($0.1f_{cu}$).

### *8.3. Modeling the interface of the concrete and the steel tube*

To model the interface of concrete core and steel tube, special interface elements were used. The interface property was chosen such that it was possible to transfer any magnitude of compression but that separation could take place without the transfer of any tensile force. A friction coefficient of $0.4N/mm^2$ was used as a property of the interface element. This value is given in BS5400.

### *8.4. Boundary conditions and loading*

In the FE model and as shown in fig. 8 the end load was applied at the rigid end plate by forces $N_1$, $N_2$ and $N_3$ such that their resultant compressive force acting on the column was applied at the required eccentricity.

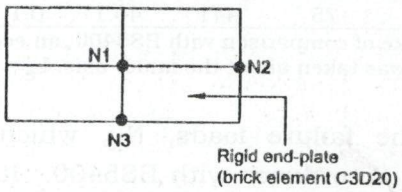


Fig. 8. Column loading.

As the column test specimens were loaded by equal end eccentricities, only half the column was modeled. The load was applied on the column nodes at the top end of the model, which was considered to be free. The boundary conditions at the column mid-height section (bottom of the FE model) are shown in fig.9, from which it can be seen that only central node 'A' is restrained in all directions. All the other nodes are restrained in Z-direction, and only the nodes that lie on the X or Y-axis are further restrained in the orthogonal direction. The displacements at the top of the FE model represent the lateral displacements and axial shortening at the column mid-height.

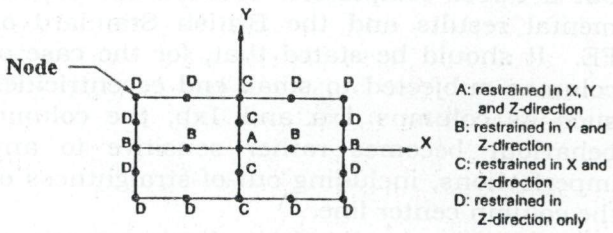


Fig.9. Boundary conditions at column mid-height.

## 9. Failure loads of columns

The results of the column tests and numerical analysis are given in table 4. The table gives the experimental failure loads, $N_e$,

Table 4
Summary of column results

| Column number | $e_x$ | Experimental | | | Finite element; FE | | | BS5400 | | |
|---|---|---|---|---|---|---|---|---|---|---|
| | | $N_e$ | $\delta_x$ | $\delta_y$ | $N_n$ | $\delta_x$* | $\delta_y$* | $N_k$ (kN) | $N_e/N_n$ | $N_e/N_k$ |
| | (mm) | (kN) | (mm) | (mm) | (kN) | (mm) | (mm) | | | |
| 1xa | 15 | 463 | 16.3 | 0.9 | 389 | 15.5 | 13.1 | 377 | 1.19 | 1.23 |
| 2xa | 30 | 347 | 23.4 | 1.4 | 341 | 27.4 | 10.1 | 321 | 1.02 | 1.08 |
| 3xa | 45 | 328 | 28.9 | 4.3 | 298 | 38.0 | 8.2 | 283 | 1.10 | 1.16 |
| 4xa | 60 | 260 | 29.1 | 2.3 | 254 | 46.2 | 4.4 | 252 | 1.02 | 1.03 |
| 1xb | 15 | 830 | 14.3 | 4.8 | 733 | 14.2 | 12.0 | 685 | 1.13 | 1.21 |
| 2xb | 30 | 693 | 21.0 | 2.1 | 647 | 21.7 | 11.2 | 589 | 1.07 | 1.28 |
| 3xb | 45 | 551 | 31.2 | 0.9 | 571 | 31.3 | 10.2 | 512 | 0.96 | 1.17 |
| 4xb | 60 | 493 | 33.7 | 1.3 | 497 | 37.9 | 8.1 | 453 | 0.99 | 1.09 |
| 5xb | 75 | 441 | 40.1 | 0.1 | 430 | 43.4 | 5.8 | 416 | 1.03 | 1.05 |

For the sake of comparison with BS5400, an eccentricity equal to 0.03B (i.e. 2.4mm for series xa and 3.0mm for series xb) was taken about the minor axis. $L_e$ = 3000mm

and also the failure loads, $N_k$, which are predicted in accordance with BS5400. It also shows that the experimental failure load $N_e$, is between 3% and 28% higher than the failure loads predicted by equation 11.3.4 in BS5400 [7]. Table 4 also shows the predicted failure loads, $N_n$, numerically calculated using the FE model. These loads are in better agreement with the experimental load. The $N_e/N_n$ ratios vary between 0.96 and 1.19 with the mean value of 1.06. The table shows that the BS5400 predictions for the studied case are generally on the safe side, as they are lower than the experimental and FE values.

It is worth mentioning here that the FE model allows for tension in concrete to be taken into account. In all calculations of predicted loads, the partial material safety factor, $\gamma_m$, was taken equal to unity in order to carry out a direct comparison between the experimental results and the British Standard or FE. It should be stated that, for the case of columns subjected to small end eccentricities such as columns 1xa and 1xb, the column behaviour becomes rather sensitive to any imperfections, including out-of-straightness of the column center line.

The mid-span in plane displacements at failure are also given in table 4. For columns subjected to major axis bending, it can be seen that the in-plane displacement at failure, $\delta_x$, increases with the increase of end eccentricity as expected. On the other hand, the transverse displacement perpendicular to the plane of bending, $\delta_y$, is seen to be rather erratic and may only be seen as an indication of whether the column failed by bending about the major or minor axis. The load-displacement relationships would seem to indicate sudden shifts in the position and direction of the mid-span neutral axis in the post-failure load-strain relationships of some of the columns that suffered sudden out-of-plane deformations. Fig. 10 shows mid-length section of column 5Xb after failure, white color clearly indicating the extent of the yielding of the steel section. Fig. 11 shows the mid-length section of column 4xb after the removal of the steel from the side of maximum compression. It can be seen from the figure that concrete remained in position despite the fact that, like all other columns, column 4xb had been loaded will into the post-failure stage. It is worth noting that, although strains of about 8000μ strain had been recorded in this side at the end of the test, the concrete is seen to have remained intact and well contained by the steel section.

## 10. Load-displacement relationships

The mid-span displacement was recorded and plotted against the load for the tested columns, and shown in figs. 12 to 19. The figures show the experimental results and also the FE results. The relationship was non-linear, characterized by an ascending branch up to failure. The descending branch was also obtained by continuous manipulation of the hydraulic jacks. The load-displacement relationships show the severe effect on the displacements as the load and eccentricity

increase. The figures clearly illustrate the adverse effect a 0.03B eccentricity about the minor axis has on the behavior of columns subjected only to a small major axis eccentricity. The other columns in the test series, which were subjected to larger major

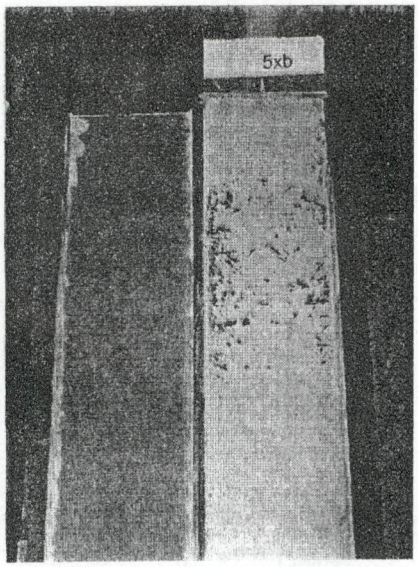


Fig. 10. Column 5xb after failure.

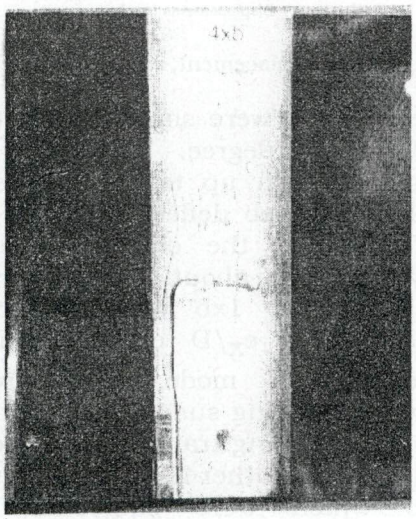


Fig. 11. Mid-span compression face of column 4xb.

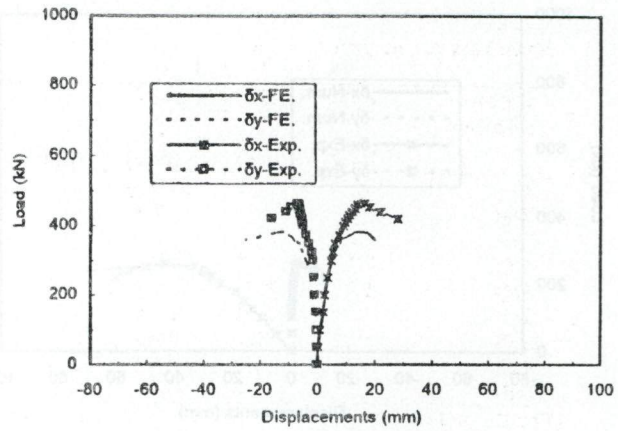


Fig. 12. Mid-length displacements; column 1×a.

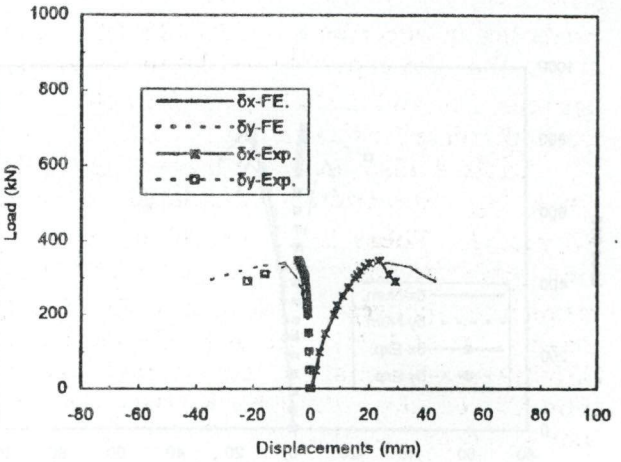


Fig. 13. Mid-length displacements; column 2×a.

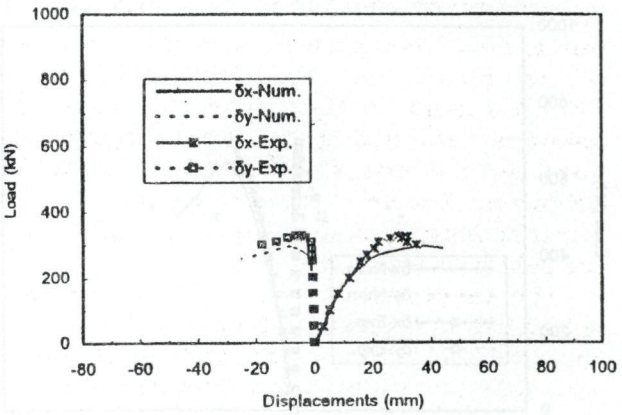


Fig. 14. Mid-length displacement; column 3×a.

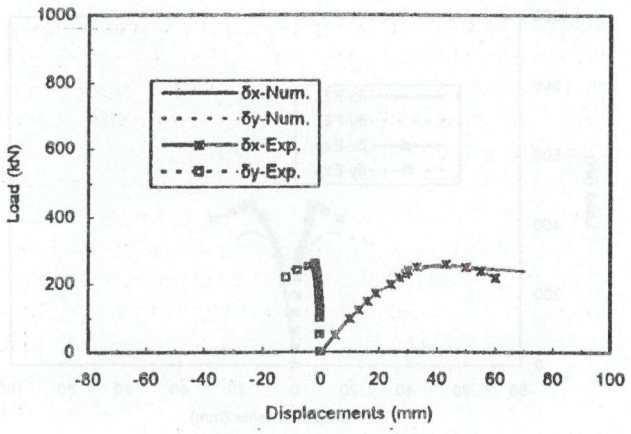


Fig. 15. Mid-length displacement; column 3×a.

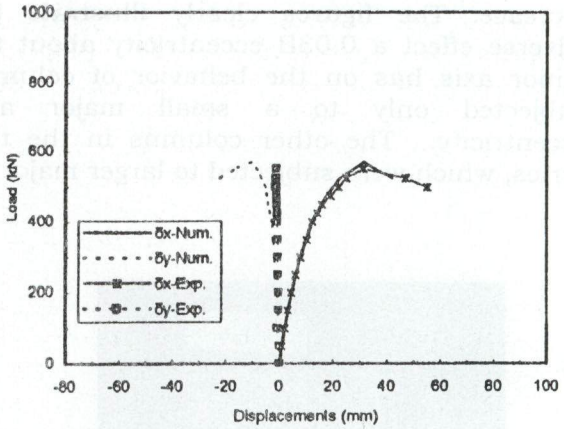


Fig. 18. Mid-length displacement; column 3×b.

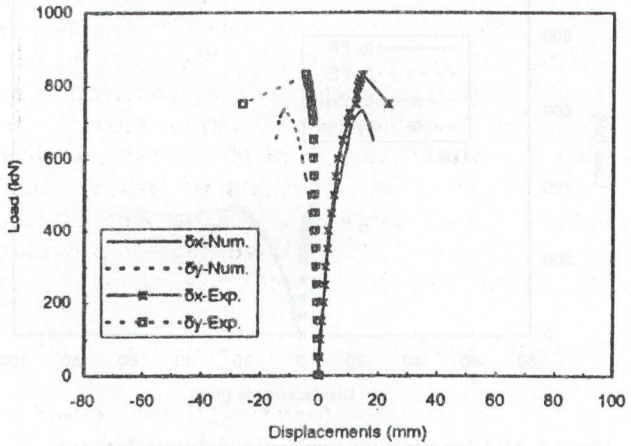


Fig. 16. Mid-length displacement; column 1×b.

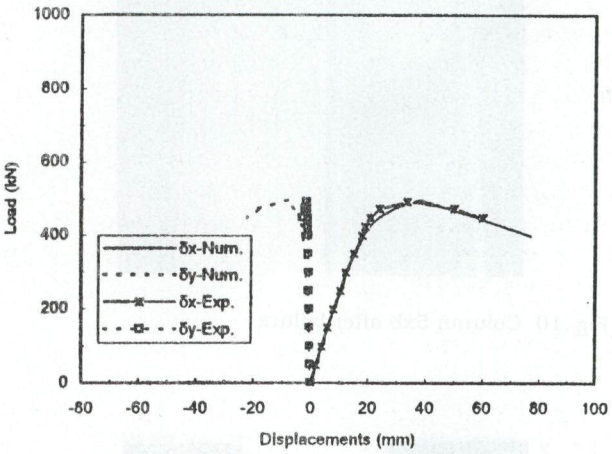


Fig. 19. Mid-length displacement; column 3×b.

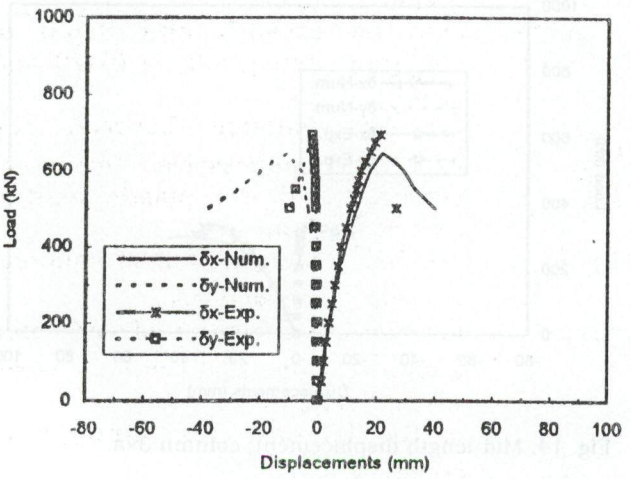


Fig. 17. Mid-length displacement; column 2×b.

axis eccentricities, were similarly affected but to a much smaller degree. The figures clearly show that although up to the failure loads column 1xa and 1xb deflected mainly in the plane of bending, the columns eventually failed by bending about the minor axes. Columns 1xa and 1xb were subjected to eccentricity ratios $e_x/D$ of 0.15 and 0.1, respectively. Their mode of failure was characterized by being sudden, and with large displacements forming transverse to the plane of bending. On the other hand, columns 4xa and 5xb which were subjected to an eccentricity ratio of 0.5, showed very little tendency for out-of-plane deformations, their lateral displacements were very small both in the pre- and post-failure stages. Compared to column 1xa, column 2xa was of the same

cross-section 100x80x5RHS, but was subjected to a relatively larger major axis eccentricity of 30mm. Figs. 12 and 13 show that, unlike column 1xa, column 2xa exhibited out-of-plane displacements before failure. Moreover, it is seen to have deformed considerably about the minor axis in the post failure stage. The transverse displacements did not, however, form suddenly as in the case of columns 1xa and 1xb, but are seen to have increased gradually until they were of a similar order to the in-plane displacements. It can be seen from table 4 that within each group the experimental failure loads decrease with the increase of the end eccentricity. It should be noted that the columns were tested in the as-received state without measuring their out-of-straightness. Such initial deformations could have a considerable effect on both the column failure load and its behavior, and could cause major differences in the load-displacement response of the various columns. Columns subjected to small major axis eccentricities are very sensitive to initial imperfections and out-of-straightness as well as any small errors in the eccentricity of the end compressive forces.

## 11. Conclusions

A numerical model using the general-purpose finite element software ABAQUS to simulate the response of composite columns of concrete filled rectangular steel hollow sections has been described. Full-scale tests were carried out to verify the model. Availability of these numerical techniques greatly increases the range of issues that can be studied economically.

For the tested specimens considered experimental investigations confirm earlier findings that BS5400 yields conservative predictions for the failure loads of concrete-filled RHS columns subjected to uniaxial bending about the major axis. However, the margin of safety of such predictions seems to decrease with the increase of the applied end eccentricity. The experimental failure loads are in better agreement with the results of the numerical analysis (FE) than that with the BS5400 predictions. The numerical work provides evidence as to the adverse effect a small minor axis eccentricity has on the behavior of columns subjected to apparently pure uniaxial bending about the major axis. This adverse effect is most noticeable in the case of long columns subjected to small end eccentricities. Such columns are also very sensitive to errors in the end eccentricities of the applied loads. The comparison between the experimental and numerical results indicate that column imperfections, such as out-of-straightness, should be measured prior to testing with a view to taking their effect into account in both the experimental and numerical analysis.

## Acknowledgments

The author wishes to thank Manchester University for allowing him to use the test rig to conduct the experiments. The authors wish to acknowledge the assistance received from, and the technical discussions carried out with, Dr Shakir khalil, of Manchester University and Mr Mike Edwards of British Steel. Special thank also goes to the Deanship of Engineering at Mutah University for providing the software for the numerical analysis.

## Nomenclature

| | |
|---|---|
| $A_c$, $A_s$ | are the cross-sectional areas of concrete and steel, respectively, |
| B, D | are the breadth and depth of steel rectangular hollow section (RHS); respectively, |
| b, d | are the breadth and depth of concrete core, given by (B-2t) and (D-2t), |
| $d_c$ | is the distance between the extreme compressive fibers of concrete and the plastic neutral axis of section, |
| $E_c$, $E_s$ | are the elastic moduli of concrete and steel; respectively, |
| $e_x$, $e_y$ | are the eccentricities of end force about major and minor axes; respectively, |
| $f_{cu}$ | is the 28 day cube strength of concrete, |
| $f_{sd}$ | is the design strength of structural steel, given by the respective |

characteristic strength divided by the material partial safety factor,

$M_{ux}$, $M_{uy}$ are the ultimate moment of resistance of composite section about major and minor axes; respectively,

$N_e$ is the experimental failure load of column,

$N_k$ is the failure load of a column predicted on the basis of BS5400

Nn is the numerically predicted failure load,

$N_u$, $N_{ue}$ are the predicted and experimental squash loads of stub column; respectively,

t is the wall thickness of rectangular hollow section,

$\delta_x$, $\delta_y$ are the experimental column mid-length displacements at failure perpendicular to major and minor axes; respectively,

$\delta_x^*$, $\delta_y^*$ are the numerically predicted column mid-length displacements at failure perpendicular to major and minor axes, respectively, and

$\rho$ is the ratio of compressive strength of concrete in bending to the design strength of steel.

**References**


[1] H. Shakir-Khalil and J. Zeghichi, "Experimental Behaviour of Concrete-Filled Rolled Rectangular Hollow-Section Columns", The Structural Engineer, Vol. 67 (19), pp. 346-353 (1989).

[2] Y. Wang and D. Moore, "A Design Method for Concrete-Filled, Hollow Section Composite Columns", The Structural Engineer, Vol. 4, pp. 368-373 (1997).

[3] V. Kodur, "Performance of High Strength Concrete-Filled Steel Columns Exposed to Fire", Canadian Journal of Civil Engineering, Vol. 25 (6) (1998).

[4] Y. Wang and V. Kodur, "An Approach for Calculating the Failure Loads of Unprotected Concrete Filled Steel Columns Exposed to Fire", Structural Engineering and Mechanics: An International Journal, Vol. 7 (2) (1999).

[5] H. Shakir-Khalil and A. Al-Rawdan, "Behaviour of Concrete-Filled Edge Columns", Third International Conference on Steel and Aluminium Structures, ICSAS", Istanbul, Turkey, pp. 515-522 (1995).

[6] H. Shakir-Khalil and A. Al-Rawdan, "Behaviour of Concrete-Filled Internal Columns", Engineering Foundation Conference on Composite Construction: Composite Construction III, Irsee, Germany (1996).

[7] BS5400, Part 5: Concrete and Composite Bridges," Code of Practice for Design of Composite Bridges, British Standards Institution (1979).

[8] DD ENV 1994-1-1 Eurocode 4, Part 1, "Design of composite steel and concrete structures, General rule and rules for buildings", British Standards Institution, London (1994).

[9] H. Shakir-Khalil and A. Al-Rawdan, "Behaviour of Asymmetrically Loaded Concrete-Filled Tubular Columns", Seventh International Symposium on Tubular Structures, Miskolc, Hungary (1996).

[10] X. Lu and Y. Yu, "Nonlinear Analysis on Concrete-Filled Rectangular Tubular Composite Columns", Structural Engineering and Mechanics: An International Journal, Vol. 10 (6) (2000)

[11] M. Saadeghvaziri, "Nonlinear modeling and evaluation of concrete-filled steel tubular columns, ABAQUS Users Conference, Milan, Italy, June (1997)

[12] Hibbitt, Karlson and Sorenson, ABAQUS Users Manual: Version 6.1 (Part 1 & 2) (2001).

[13] H. Shakir-Khalil, "Push-Out Strength of Concrete-Filled Steel Hollow Sections", The Structural Engineer, Vol. 71 (13), pp. 230-233 (1993).


Received December 10, 2001
Accepted July 13, 2002